Journal of Neuroinflammation

RESEARCH

Open Access

Tryptophan-rich diet and its effects on Htr7$^+$ Tregs in alleviating neuroinflammation and cognitive impairment induced by lipopolysaccharide

Dinghao Xue[1,2†], Xu Guo[1†], Jingjing Liu[1,3†], Yanxiang Li[4], Luyu Liu[1], Guosong Liao[1], Mingru Zhang[2], Jiangbei Cao[1], Yanhong Liu[1], Jingsheng Lou[1], Hao Li[1], Weidong Mi[1], Long Wang[5*†] and Qiang Fu[1*†]

Abstract

Background Neuroinflammation is a vital pathogenic mechanism for neurodegenerative diseases such as Alzheimer's, schizophrenia, and age-related cognitive decline. Regulatory T cells (Tregs) exhibit potent anti-inflammatory properties and can modulate neurodegenerative diseases arising from central nervous system inflammatory responses. However, the role of Tregs in neuroinflammation-related cognitive dysfunction remains unclear. It is highly plausible that Htr7$^+$ Tregs expressing unique genes associated with the nervous system, including the Htr7 gene encoding the serotonin receptor 5-HT$_7$, play a pivotal role.

Methods Mice were given a tryptophan-rich diet (with a tryptophan content of 0.6%) or a normal diet (with a tryptophan content of 0.16%). The neuroinflammation-mediated cognitive dysfunction model was established by intracerebroventricular injection of lipopolysaccharide (LPS) in 8-week-old C57BL/6J mice. The activation and infiltration of Tregs were measured using flow cytometry. Primary Tregs were cocultured separately with primary CD8$^+$ T cells and primary microglia for in vitro validation of the impact of 5-HT and 5-HT$_7$ receptor on Tregs. Prior to their transfer into recombination activating gene 1 (Rag1$^{-/-}$) mice, Tregs were ex vivo transfected with lentivirus to knock down the expression of Htr7.

Results In this study, the tryptophan-rich diet was found to reverse LPS-induced cognitive impairment and reduce the levels of 5-HT in peripheral blood. The tryptophan-rich diet led to increased levels of 5-HT in peripheral blood, which in turn promoted the proliferation and activation of Htr7$^+$ Tregs. Additionally, the tryptophan-rich diet was also shown to attenuate LPS-mediated neuroinflammation by activating Htr7$^+$ Tregs. Furthermore, 5-HT and 5-HT$_7$

†Dinghao Xue, Xu Guo and Jingjing Liu contributed equally to this work.

†Long Wang and Qiang Fu contributed equally to this work.

*Correspondence:
Long Wang
flynn.xu@163.com
Qiang Fu
dr_fuqiang@hotmail.com

Full list of author information is available at the end of the article

receptor were found to enhance the immunosuppressive effect of Tregs on $CD8^+$ T cells and microglia. In $Rag1^{-/-}$ mice, $Htr7^+$ Tregs were shown to alleviate LPS-induced neuroinflammation and cognitive impairment.

Conclusions Our research revealed the ability of $Htr7^+$ Tregs to mitigate neuroinflammation and prevent neuronal damage by suppressing the infiltration of $CD8^+$ T cells into the brain and excessive activation of microglia, thereby ameliorating LPS-induced cognitive impairment. These insights may offer novel therapeutic targets involving Tregs for neuroinflammation and cognitive impairment.

Keywords Cognitive dysfunction, Regulatory T cells, Serotonin, Neuroinflammation, Lipopolysaccharide

Introduction

Neuroinflammation, a part of systemic immune response, is characterized by increased oxidative stress, elevated pro-inflammatory cytokine expression, and activated microglia. The consequences of neuroinflammation depend on the primary cause, as well as the intensity and duration of inflammation. Prolonged, uncontrolled inflammation is destructive, leading to neuronal dysfunction ultimately [1]. Neuroinflammation plays a crucial role in neurodegenerative diseases such as Alzheimer's, schizophrenia, and age-related cognitive decline [2–4]. Numerous factors can trigger neuroinflammation, such as anesthesia and surgical stimulation, which can induce potent central and peripheral inflammatory responses, leading to cognitive impairment in animals as peripheral immune cells migrate to the brain and upregulate pro-inflammatory cytokines and mediators in the central nervous system [5, 6]. Nevertheless, the exact pathological mechanisms by which neuroinflammation affects cognitive function remain elusive. In animal models, systemic and intracerebroventricular administration of lipopolysaccharide (LPS) can induce cognitive impairment [7, 8]. Studies suggested that neuroinflammatory response plays a critical role in LPS-induced memory impairment in mouse models. Alleviating hippocampal inflammation can improve learning and memory deficits in mice [9].

Regulatory T cells (Tregs) are vital components of the immune system that function to maintain immune homeostasis and limit excessive inflammatory responses, thereby protecting the body from inflammatory damage [10]. Tregs secrete inhibitory inflammatory factors such as IL-10 and TGF-β, which suppress the activation of effector cells, including T and B lymphocytes, macrophages, and dendritic cells, and inhibit their infiltration into effector brain regions. Tregs that infiltrate the brain can also exert immunosuppressive effects, possibly by modulating the survival conditions of cytotoxic T cells, leading to their apoptosis [11]. In their study, Tian et al. discovered significant infiltration of Tregs in the hippocampal region, with upregulation of IL-10 mRNA expression, indicating their role in suppressing immune responses [12]. Minako et al. conducted a systematic investigation of Tregs and reported that a specific subtype of Tregs express the receptor 5-HT_7 for 5-hydroxytryptamine (5-HT), also known as serotonin. Binding 5-HT to 5-HT_7 receptor stimulates the proliferation of $Htr7^+$ Tregs and enhances their immune activity. $Htr7^+$ Tregs proliferate in the cervical lymph nodes and can also infiltrate effector brain regions, where they exert immunosuppressive effects [13]. Approximately 90% of 5-HT in the human body is produced in the intestine, and 5-HT is synthesized in enterochromaffin cells and the enteric nervous plexus. Through enzymatic catalysis in intestinal cells, tryptophan is converted to 5-HT in the gut. Furthermore, studies have indicated that certain microbial communities in the gut play pivotal roles in the synthesis of 5-HT [14]. A diet rich in tryptophan can increase 5-HT levels in peripheral blood [15]. Hence, we can try to modulate $Htr7^+$ Tregs by augmenting peripheral blood levels of 5-HT in mice through the administration of a diet rich in tryptophan.

Accordingly, we hypothesize that $Htr7^+$ Tregs is associated with neuroinflammation induced cognitive dysfunction. To test this hypothesis, we assessed the impact of $Htr7^+$ Tregs on neuroinflammation and cognitive function following intracerebroventricular administration of LPS, aiming to explore potential Tregs-based therapeutic strategies for neuroinflammation-mediated cognitive dysfunction.

Materials and methods

Animals

Male C57BL/6J WT mice aged 8 weeks (weighing 22 to 25 g) and C57BL/6J WT neonatal mice aged 24 h (weighing 9 to 11 g) were obtained from the Beijing SPF Animal Technology Company. $Rag1^{-/-}$ mice (B6.129S7-Rag1tm1Mom/J) on the C57BL/6 background were originally purchased from The Jackson Laboratory. The mice were housed in a carefully regulated environment with standard temperature and humidity levels to ensure their well-being and minimize any potential stressors. The animals were given free access to food and water throughout the duration of the experiment, allowing them to maintain their normal nutritional intake. All animal experiments were approved by the Ethics Committee for Animal Experimentation of the Chinese PLA General Hospital.

Intracerebroventricular microinjection surgery

Prior to the stereotactic injection of LPS (*Escherichia coli* serotype 0111:B4, Sigma–Aldrich, St. Louis, USA) or artificial cerebrospinal fluid (aCSF), the mice were anesthetized by an intraperitoneal injection of Avertin (200 mg/kg). Specific coordinates (posterior: 0.5, lateral: ± 1.0, and ventral: 2.0 from the bregma [in mm]) were used to precisely locate the lateral ventricle for the injection. Subsequently, LPS or aCSF was administered at a consistent rate within a 3-minute time frame. Following the injection, the needle was maintained in position for a minimum of 3 min.

Five days after the Morris water maze (MWM) training phase, LPS (2 μg of LPS dissolved in 2 μL of aCSF [containing 140 mM NaCl, 3.0 mM KCl, 2.5 mM $CaCl_2$, 1.2 mM Na_2HPO, and 41.0 mM $MgCl_2$]) was intracerebroventricularly injected. The control groups were administered an equivalent volume of aCSF.

Experimental diets

Based on previous studies [15], we fed the mice a similar tryptophan-rich diet. All mice were nourished with diets conforming to the AIN-93 M (3.872 kcal/g), comprising 17.56% kcal of protein, 70.82% kcal of carbohydrates, and 11.62% kcal of fat (HFK Bioscience, Beijing, China). The Sham group, the Sham+Trp group, the LPS group, and the LPS+Trp group were treated as follows: the Sham group and the LPS group contained 0.16% tryptophan. Meanwhile, the Sham+Trp group and the LPS+Trp group contained 0.6% tryptophan.

Open filed test (OF test)

To examine whether LPS injection had an effect on spontaneous activity in mice, open field testing was performed 24 h post-treatment. The testing room was divided into 16 areas, with mice placed in a corner to freely explore for 2 min. Numbers of line crossing and total distance were recorded for 8 min. The area was cleaned with 75% ethanol post-testing to remove potential interferences.

MWM test

The MWM test was conducted in a large circular pool filled with water and featuring a circular hidden platform, serving as the basis for evaluating spatial learning and memory in mice. The pool was then provided visual cues to aid the mice in remembering the platform's location. The test comprised place navigation trials and a spatial probe test. Following daily training sessions, the latency of the mice to find the platform was recorded and averaged. After five days of navigation training, the mice received intracerebroventricular microinjections. The following day, the hidden platforms were removed, and the spatial probe test began, during which the mice were allowed to access the platform. The latency from entering the water maze to reaching the original platform, the percentage of time spent in different quadrants, the swimming speed, and the movement trajectory of mice in the water maze were recorded throughout the experiment.

Primary cell coculture

Isolate primary Tregs and inoculate them into a 12-well plate containing complete RPMI-1640 medium supplemented with 10ng/mL IL-2 and TNF-α, followed by a 24-hour incubation period. Subsequently, combine carboxyfluorescein succinimidyl ester (CFSE)-labeled primary $CD8^+$ T cells with irradiated antigen-presenting cells (APCs) (spleen cells depleted of T lymphocytes) and co-culture with soluble anti-mouse CD3 antibody (Abcam, ab237721) at a concentration of 0.5 μg/mL. After 72 h of co-culture, evaluate CFSE dilution through flow cytometry analysis.

T_{eff} (primary $CD8^+$ T cells or primary microglia) with irradiated APCs (spleen cells depleted of T lymphocytes) and co-culture with soluble anti-mouse CD3 antibody at a concentration of 0.5 μg/mL, then Tregs, stimulated by IL-2 and TNF-α for 24 h, were added to the wells at a desired ratio (Teff: Treg=1:1). After 4 h of coculture in a cell culture incubator, the cells were divided into PBS, 5-HT, and 5-HT+SB269970 (5-HT+SB) groups. SB269970 (Abcam, ab120508, Cambridge, UK) is a selective inhibitor of $5\text{-}HT_7$ receptor [16]. The PBS group received PBS, the 5-HT group received 5-HT, and the 5-HT+SB group received both 5-HT and SB269970 for an additional 24 h. Then qRT-PCR, Western lotting, and flow cytometry were performed. Drug concentrations were 8.3 nM/mL for 5-HT and 200 ng/mL for SB269970.

Flow cytometry

The cervical lymph nodes were gently mechanically ground using glass slides with frosted edges, followed by washing the slides with PBS solution and filtering the liquid through a 70 μm mesh filter to obtain a single-cell suspension. For brain tissue, prepare a single-cell suspension according to the manufacturer's instructions using a neural tissue dissociation kit (Miltenyi Biotec, 130-093-231).

The antibodies and detection kits used were from several companies: CD4, CD25 and Foxp3 (stained with a mouse Regulatory T Cell Staining Kit), Anti-Mouse CD206 PE, Anti-Mouse MHC-II FITC, Anti-Mouse MHC-I FITC, Rat IgG2a Isotype Control PE, Rat IgG2a Isotype Control FITC, Rat IgG1 Isotype Control APC, Armenian Hamster IgG Isotype Control Percp-Cyanine 5.5, Anti-mouse/human CD44, Anti-mouse CD62L, Anti-Mouse CD45 Percp-Cyanine 5.5, and Anti-Mouse CD11b APC were from eBioscience (Waltham, MA, USA); Carboxyfluorescein diacetate succinimidyl ester (CFSE) was from Absin Biology (Shanghai, China);

Anti-Mouse 5-HT7 was from Novus Biologicals (Littleton, CO, USA); and the Annexin V-FITC Apoptosis Staining/Detection Kit was from Abcam (Cambridge, UK). Flow cytometry data acquired from a FACS Calibur (BD Biosciences, FACSCanto II, San Jose, CA, USA) were subjected to analysis using FlowJo V10 software.

Annexin V staining

Cells were isolated and centrifuged to collect a pellet, which was washed with PBS, then resuspended in diluted binding buffer. The cells were adjusted to a concentration of 5×10^6 cells/mL and incubated with Annexin V/FITC. Propidium iodide (PI) and PBS were added for flow cytometry analysis.

Lentiviral transfection of Tregs

Htr7 downregulation was achieved by transfecting lentiviral particles expressing a Flag epitope-tagged form of murine protein into Tregs from cervical lymph nodes 72 h before the experiments. pSLenti-EF1-EGFP-CMVCHRNA7(GV417)-3FLAG (denoted as the empty vector) was used as a control lentivirus. Htr7 downregulation was achieved by transfecting Tregs with lentivirus expressing Htr7-specific short hairpin RNAs (shHtr7) 72 h before the experiments. A lentiviral vector expressing a scrambled sequence (shScramble) was used as a control shRNA. The lentiviral vectors containing Htr7-Flag, the empty vector, shHtr7, and shScramble were purchased from Obio (Shanghai, China).

Adoptive cell transfer in Rag1-/- mice

Tregs isolated from healthy mice cervical lymph nodes via magnetic sorting (Miltenyi, Germany) were plated at 5×10^5 cells/well in a 24-well plate and stimulated with anti-CD3/CD28 beads (Miltenyi, Germany) for 48 h. After transfection with the Htr7-Flag lentivirus to downregulate Htr7 expression, 2×10^6 transfected $Htr7^+$ Tregs and $CD4^+CD25^-$ T cells were injected via the femoral vein into recipient $Rag1^{-/-}$ mice before the MWM test. The $Rag1^{-/-}$ mice were randomly divided into four groups: the Sham group (aCSF + $CD4^+CD25^-$ T cells), the LPS group (LPS + $CD4^+CD25^-$ T cells), the LPS + Treg group (LPS + Tregs transfected with empty vector + $CD4^+CD25^-$ T cells), and the LPS + $Treg^{shHtr7}$ group (LPS + Tregs transfected with Htr7-Flag + $CD4^+CD25^-$ T cells). Mice were treated with LPS or aCSF via intracerebroventricular injection.

Western blotting

For the Western blot analysis, equimolar quantities (40 μg) of total protein per sample were separated via SDS–PAGE on a 12.5% gel. The proteins were subsequently transferred onto a polyvinylidene fluoride membrane using the semidry blotting technique. The membrane was then subjected to an extended overnight blocking phase at 4 °C utilizing a 5% BSA solution. Subsequently, the membrane was incubated with primary antibodies against the proteins of interest: perforin (1:1000, Abcam, ab97305, Cambridge, UK) and granzyme B (1:3000, Abcam, ab255598, Cambridge, UK). The membranes were incubated with these antibodies at ambient temperature for 2.5 h. After the necessary washes were performed, the membranes were incubated with horseradish peroxidase (HRP)-conjugated anti-rabbit secondary antibody (1:10,000, Abcam, ab107866, Cambridge, UK). The images were subjected to analysis using HIN ImageJ software and were presented as the density ratio relative to that of β-actin.

Antibodies for immunofluorescence staining

The primary antibodies used for immunofluorescence staining were as follows: rabbit anti-CD8 (1:500, Servicebio, P01731), mouse anti-Iba-1 (1:500, Servicebio, O70200), rabbit anti-Ly6g (1:200, Servicebio, P35461), rabbit anti-CD3 (1:50, Abcam, ab135372), rabbit anti-myelin basic protein (MBP, 1:500, Abcam, ab40390), and mouse anti-nonphosphorylated neurofilaments (SMI32, 1:1000, Biolegend, 801701). The secondary antibodies used for immunohistochemical staining were purchased from Invitrogen.

Quantitative real-time PCR (qRT–PCR)

The cellular specimens were subjected to total RNA extraction using an RNA extraction kit (Solarbio, R1200, Beijing, China). A universal reverse transcription kit (Solarbio, RP1105, Beijing, China) was subsequently used for reverse transcription. Real-time PCR was carried out using a universal RT−PCR kit (Solarbio, RP1200, Beijing, China) on a Step One Plus thermal cycler (Thermo Fisher, 4376592, Waltham, MA, USA). The primers used were designed according to the principles of primer design, and their specific sequences can be found in Table 1.

Enzyme-linked immunosorbent assay (ELISA)

The concentrations of IL-10 (Thermo Fisher Scientific, 88-7105-22, Minneapolis, MN, USA), TGF-β (Thermo Fisher Scientific, 88-8350-22, Minneapolis, MN, USA), TNF-α (Thermo Fisher Scientific, 88-7324-22, Minneapolis, MN, USA), and IL-1β (Thermo Fisher Scientific, 88-7013-22, Minneapolis, MN, USA) were determined using ELISA kits. Hippocampal tissues were carefully disrupted in a solution of RIPA lysis buffer. Subsequently, the resultant mixture was subjected to centrifugation at a speed of 12,000 rotations/min for 5 min, maintaining a frigid temperature of 4 °C. Through this process, the protein fraction in the supernatant was effectively isolated. The subsequent experimental procedures strictly adhered to the guidelines provided by the manufacturer. To

Table 1 Primer sequences used for qRT-PCR analysis

Primer Name	Forward Primer (5′-3′)	Reverse Primer (5′-3′)
Perforin	CAAGGTAGCCAATTTTGCAGC	GTACATGCGACACTCTACTGTG
Granzyme B	GCCCCACTCTCGACCCTA	AGCACAAAGTCCTCTCGAAT
IL-1β	ACTCATTGTGGCTGTGGAGA	TTGTTCATCTCGGAGCCTGT
iNOS	CACAGTGTCGCTGGTTTGAA	TCTCCGTGGGGCTTGTAGT
IL-4	GGTCTCAACCCCCAGCTAGT	GCCGATGATCTCTCTCAAGTGAT
TNF-α	CTCATGCACCACCATCAAGG	ACCTGACCACTCTCCCTTTG

determine the concentrations of IL-10, TGF-β, TNF-α, and IL-1β, spectrophotometric analysis was conducted, and the absorbance was measured at a wavelength of 450 nm. Utilizing a standard curve, the exact concentrations of the aforementioned proteins were accurately determined.

Statistical analyses

All the results were meticulously scrutinized by an assessor who was blinded to the experimental design. The findings are presented as the mean ± standard error of the mean (SEM) for continuous numerical variables. The difference between two groups was evaluated using Student's *t* test. For comparisons among multiple groups, either a one- or two-way analysis of variance (ANOVA) was used, followed by a Tukey post hoc analysis. To evaluate the differences between various groups at each time point, two-way ANOVA with a subsequent Tukey post hoc test was conducted. The statistical analyses were performed using GraphPad Prism 9.5 (GraphPad Software, Inc., San Diego, CA, USA). All the statistical tests were two-tailed, and a significance level of $P<0.05$ was considered to indicate statistical significance.

Results

Tryptophan-rich diet reversed LPS-induced cognitive impairment and decreased 5-HT in peripheral blood

Our prior work has demonstrated that intracerebroventricular injection of LPS results in learning and memory deficits [17]. Therefore, the present study assessed the protective effects of the tryptophan-rich diet against LPS-induced memory impairment in mice.

Mice were administered either the tryptophan-rich diet or the normal diet for 41 days after two weeks of adapt feeding. After a 35-day dietary intervention, the Sham + Trp group and the LPS + Trp group followed a diet rich in tryptophan, while the Sham group and the LPS group maintained a normal diet, we performed a five-day MWM test training phase. The LPS group and the LPS + Trp group of mice were subsequently subjected to intracerebroventricular injection of LPS. The Sham group and the Sham + Trp group received an equal volume of aCSF. The MWM probe test was performed 24 h after intracerebroventricular microinjection (Fig. 1A).

The results of the MWM test revealed that during the training phase of the MWM test, the proficiency of the mice in locating the hidden platform was enhanced with training. There were no notable distinctions in the latency to reach the platform across the groups on a daily basis ($F_{(3,\ 24)}=0.2630$, $P=0.8514$, Fig. 1B, E). The probe test was performed 24 h after LPS administration. During the probe test, all four groups of mice displayed a noteworthy preference for the target quadrant, dedicating significantly more time to the target quadrant than to the opposite quadrant. However, the LPS group exhibited a discernible decrease in the duration spent in the target quadrant, which was different from that of the other three groups ($F_{(3,\ 24)}=5.619$, $P=0.0046$, Fig. 1C, E). The swimming velocities exhibited by the mice were comparable across all groups, effectively excluding any potential effect of motor or perceptual factors on spatial learning and memory ($F_{(3,\ 24)}=0.2477$, $P=0.8621$, Fig. 1D). This suggested that intracerebroventricular LPS treatment disrupted the memory of the shortest path and the location of the platform in mice. Moreover, the tryptophan-rich diet was found to alleviate cognitive dysfunction in mice induced by LPS without affecting the motor abilities and cognitive functions of sham mice.

Considering the profound effects of LPS-induced neuroinflammation on the intricate mechanisms of the gut-brain axis, we evaluated the concentrations of 5-HT, the tryptophan metabolite synthesized in the intestines of mice. The HPLC–MS technique was used to assess the levels of 5-HT in the peripheral blood, hippocampal regions and colon tissue of mice following intracerebroventricular injection. Notably, compared to the other three groups, the Sham + Trp group showed a significant increase in serum 5-HT levels, while the LPS group exhibited a significant decrease in peripheral blood 5-HT concentrations in mice ($F_{(3,\ 24)}=16.49$, $P<0.0001$, Fig. 1F). However, there was no significant difference in the concentration of 5-HT in the hippocampal region among the four groups of mice ($F_{(3,\ 24)}=0.4892$, $P=0.6930$, Fig. 1G). Moreover, the levels of 5-HT in colon were higher in the Sham + Trp group than those in the other three groups, whereas the LPS group showed a significant reduction in 5-HT concentrations in the colon of the mice ($F_{(3,\ 24)}=22.06$, $P<0.0001$, Fig. 1H). This is consistent with the peripheral blood 5-HT related findings.

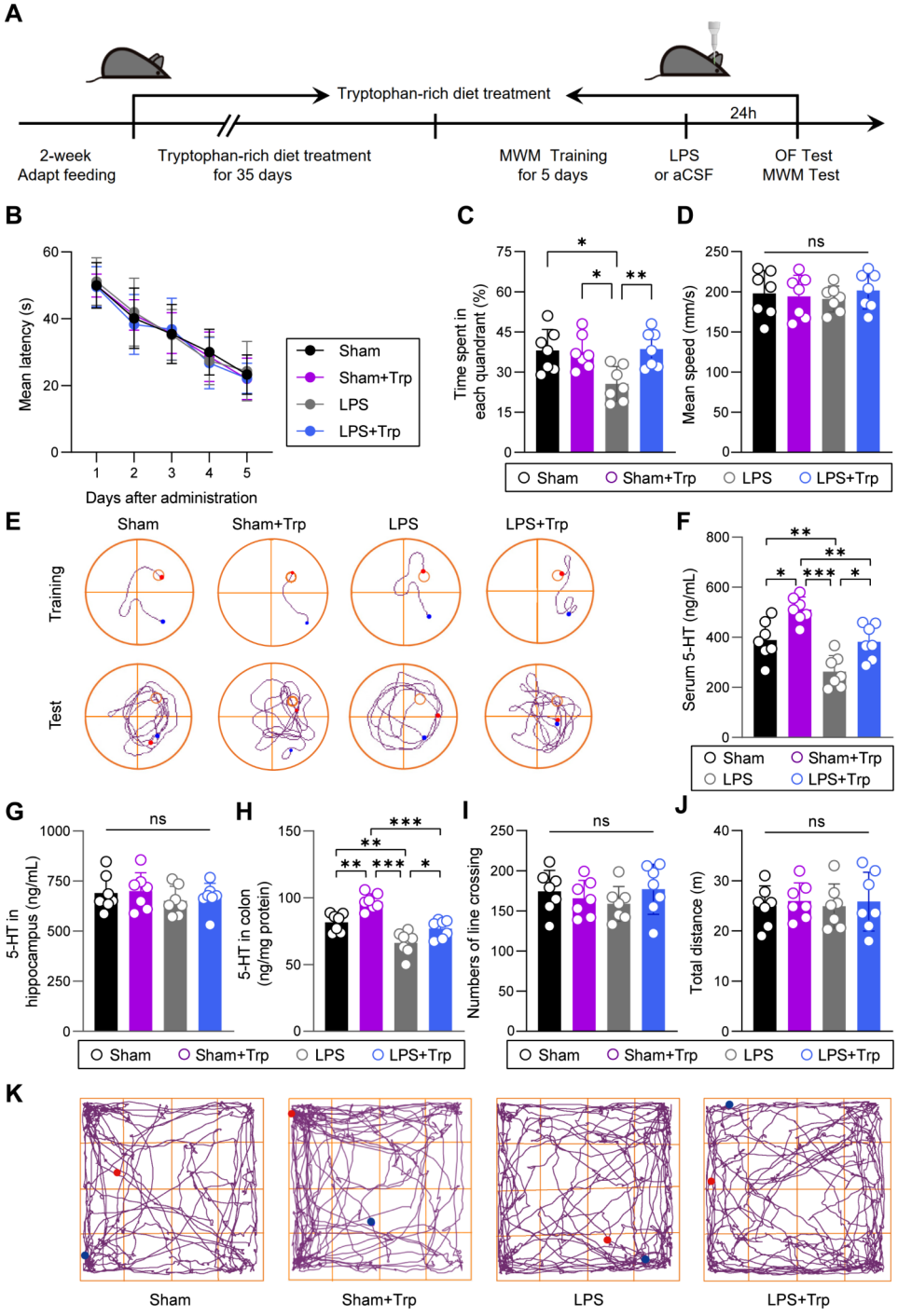

Fig. 1 Tryptophan-rich diet reversed LPS-induced cognitive impairment and decreased 5-HT in peripheral blood. **A** Flowchart illustrates the experimental design. **B** Mean escape latency to reach the hidden platform during the 5-day training ($n=7$/group). **C** The percentage of time spent in the target quadrant ($n=7$/group). **D** The mean swimming velocity exhibited by each experimental group during the probe test ($n=7$/group). **E** Representative trace graphs during the MWM test. **F-H** 5-HT concentration in serum (**F**), hippocampus (**G**) and colon (**H**) in mice after LPS treatment ($n=7$/group). **I** Numbers of line crossing ($n=7$/group). **J** Total distance ($n=7$/group). **K** Representative moving trajectories of mice in the open arena during the 8 min. The green spot presents the start of mice movement, and the red spot presents the end. $^{*}P<0.05$, $^{**}P<0.01$, $^{***}P<0.001$, ns indicates nonsignificant

This suggested that intracerebroventricular injection of LPS may affect the synthesis of intestinal 5-HT, thereby leading to a decrease in peripheral blood 5-HT levels. However, supplemental tryptophan can elevate the levels of 5-HT in both the colon and peripheral blood of both sham and experimental mice. In the OF test, before MWM probe test, there were no significant differences in the number of line crossings ($F_{(3,\ 24)}=0.7297$, $P=0.5444$,

Fig. 1I, K) and total distance ($F_{(3, 24)}$=0.1049, P=0.9564, Fig. 1J, K) among the four groups of mice, indicating that the differences observed in the MWM test were not due to a reduction in spontaneous activity caused by the mice becoming sick as a result of LPS treatment. These findings suggested that LPS may potentially impact cognitive function by affecting the biosynthesis of 5-HT within the gut, consequently leading to a reduction in peripheral blood serotonin levels.

The elevation of peripheral blood 5-HT levels induced by the tryptophan-rich diet promoted the proliferation and activation of Htr7$^+$ Tregs

Given the profound impact of intracerebroventricular injection of LPS on immune function, we evaluated the percentage of Tregs in the cervical lymph nodes and brain 24 h after LPS treatment by flow cytometry. There was no discernible difference in the proportion of Foxp3$^+$CD25$^+$ Tregs among the four groups ($F_{(3, 24)}$=0.08744, P=0.9662, Fig. 2A, B). However, compared with the other groups, the fraction of Htr7$^+$ Tregs in the cervical lymph nodes was higher in the Sham+Trp group, while it was lower in the LPS group ($F_{(3, 24)}$=15.81, P<0.0001, Fig. 2A, C). Flow cytometry analysis of brain-infiltrating Tregs revealed a decrease in Foxp3$^+$CD25$^+$ Tregs ($t_{(12)}$=3.841, P=0.0023) and Htr7$^+$ Tregs ($t_{(12)}$=2.821, P=0.0154) in the LPS group compared to those in the LPS+Trp group (Fig. 2D-F). These findings indicated that microinjection of LPS leads to central inflammatory responses and disruptions in the synthesis of 5-HT, which inhibit the proliferation and activation of peripheral Htr7$^+$ Tregs while also suppressing their infiltration into the brain. However, the administration of the tryptophan-rich diet to mice to increase peripheral blood 5-HT levels can promote the proliferation of peripheral Htr7$^+$ Tregs and their infiltration into the central nervous system. It is worth noting that providing the diet rich in tryptophan to sham mice promotes the proliferation of Htr7$^+$ Tregs in their cervical lymph nodes without affecting such cells in their brains.

To assess the immunosuppressive activity of infiltrating Htr7$^+$ Tregs in the brain, we employed immunofluorescence and flow cytometry to examine the infiltration of CD8$^+$ T lymphocytes in the brains of the mice. Immunofluorescence revealed a significant increase in the number of infiltrating CD8$^+$ T cells in the dentate gyrus (DG) of the hippocampus in the LPS group compared to that in the LPS+Trp group ($t_{(12)}$=4.166, P=0.0013, Fig. 2G, H). Similar findings were observed via flow cytometry, which also demonstrated a markedly greater proportion of infiltrating CD44^{high}CD62L^{low}CD8$^+$ T lymphocytes in the hippocampal DG of mice in the LPS group than in those in the LPS+Trp group ($t_{(12)}$=2.754, P=0.0175; Fig. 2I, J). These findings suggested that the increase in peripheral blood 5-HT levels induced by the tryptophan-rich diet facilitated the activation of Htr7$^+$ Tregs, enhancing their immunosuppressive activity.

Tryptophan-rich diet attenuated LPS-mediated neuroinflammation by activating Htr7+ Tregs

As is well-known, the activation of mature T lymphocytes, neutrophils, and microglia constitutes a response to neuroinflammation, and intense neuroinflammatory damage can result in demyelination of neurons. Therefore, we utilized immunofluorescence and ELISA to assess the inflammatory response in the hippocampal region of mice 24 h after LPS injection. CD3 is expressed on the surface of almost all mature T lymphocytes. The immunofluorescence results revealed a significant increase in the activation of CD3$^+$ T cells in the DG of the hippocampus in the LPS group compared to the other three groups ($t_{(12)}$=2.550, P=0.0255, Fig. 3A, B). Additionally, the accumulation of neutrophils in the hippocampal DG was more pronounced in the LPS group than in the other three groups ($t_{(12)}$=2.495, P=0.0282, Fig. 3A, C). Moreover, compared to those in the remaining three groups, the LPS group exhibited increased Iba-1 staining in the DG of the hippocampus, which was indicative of a noteworthy increase in microglial activation ($t_{(12)}$=2.251, P=0.0439, Fig. 3A, D). The SMI-32/MBP protein ratio is a widely acknowledged parameter for assessing demyelination. We observed a significant increase in demyelination of neurons in the hippocampal region in mice in the LPS group compared to those in the other three groups ($t_{(12)}$=2.263, P=0.0430, Fig. 3A, E).

The levels of two common anti-inflammatory cytokines (IL-10 and TGF-β) released by Tregs in conjunction with TNF-α and IL-1β (two common proinflammatory cytokines) in the hippocampal region were evaluated through ELISA. Compared to those in the other three groups, the IL-10 levels in the hippocampal region were significantly lower in the LPS group ($F_{(3, 24)}$=6.178, P=0.0029, Fig. 3F). Furthermore, in comparison to those in the other three groups, the hippocampal TGF-β levels in the LPS group were notably lower ($F_{(3, 24)}$=6.090, P=0.0031, Fig. 3G). Conversely, in contrast to those in the other three groups, TNF-α levels in the hippocampal region were greater in the LPS group ($F_{(3, 24)}$=4.976, P=0.0080, Fig. 3H). Similarly, compared to those in the other three groups, the IL-1β levels in the hippocampal region were elevated in the LPS group ($F_{(3, 24)}$=10.59, P=0.0001, Fig. 3I). Collectively, our results suggested that LPS injection induces central inflammatory injury, which can be mitigated through the activation of Htr7$^+$ Tregs.

5-HT and 5-HT$_7$receptor enhanced the immunosuppressive effect of Tregs on CD8$^+$T cells and microglia.

To determine the mechanism by which 5-HT activates the immunosuppressive effect of Tregs, a series of cellular experiments was conducted. We utilized CFSE to

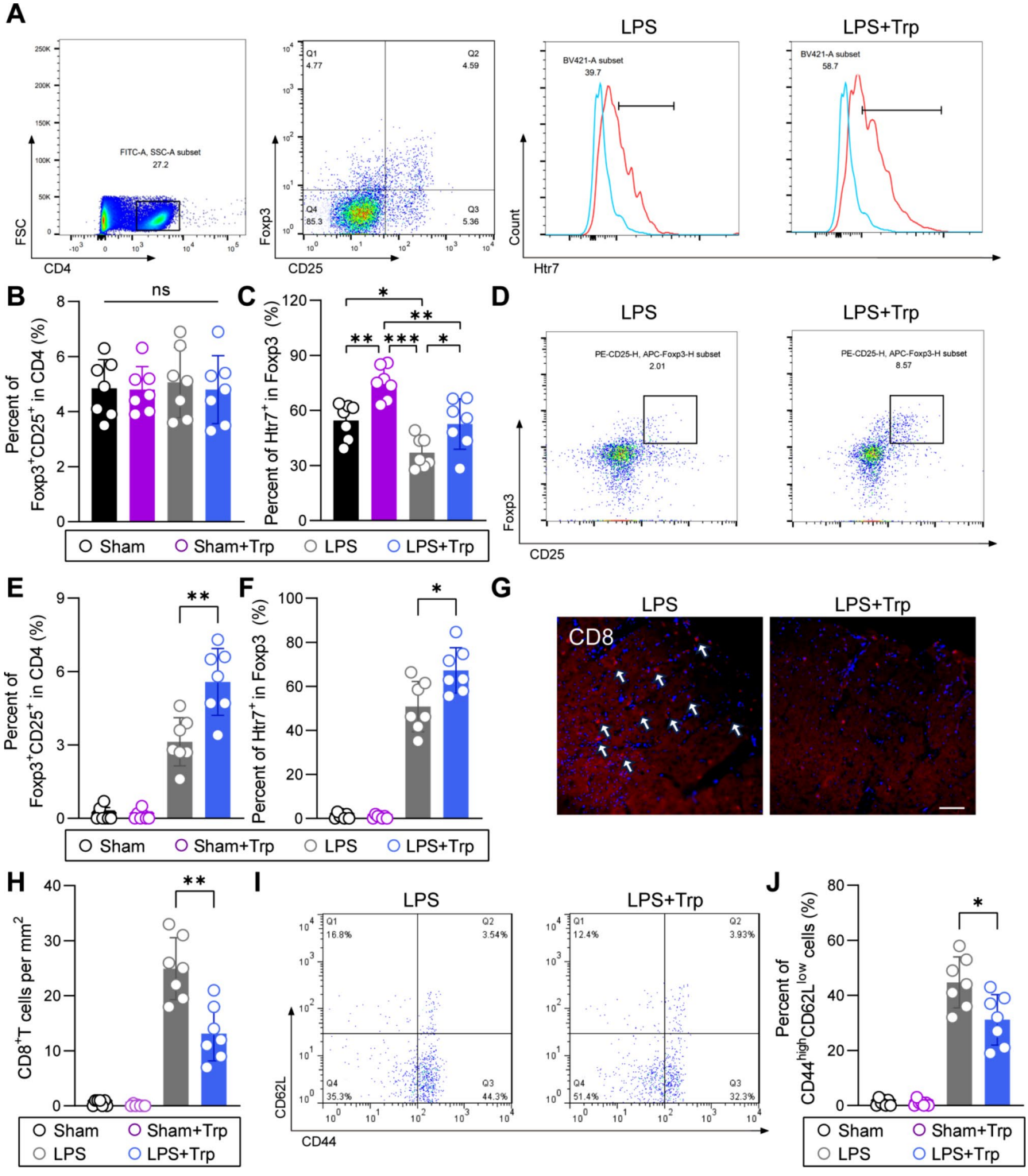

Fig. 2 The elevation of peripheral blood 5-HT levels induced by the tryptophan-rich diet promoted the proliferation and activation of Htr7$^+$ Tregs. **A-C** Representative dot plots, histogram (**A**) and percentages of Tregs (**B**) and Htr7$^+$ Tregs (**C**) detected via flow cytometry in the cervical lymph nodes ($n = 7$/group). **D-F** Representative dot plots (**D**) and percentages of Tregs (**E**) and Htr7$^+$ Tregs (**F**) detected via flow cytometry in the hippocampus ($n = 7$/group). **G** Representative images of CD8 immunostaining in the hippocampal DG. Scale bar = 200 μm. **H** Quantification of CD8$^+$ cells ($n = 7$/group). **I**, **J** Representative dot plots (**I**) and the percentages of CD44^{high}CD62L^{low} cells on CD8$^+$ T lymphocytes determined via flow cytometry (**J**) in the hippocampal DG 24 h after LPS treatment ($n = 7$/group). $^*P < 0.05$, $^{**}P < 0.01$, $^{***}P < 0.001$, ns indicates nonsignificant

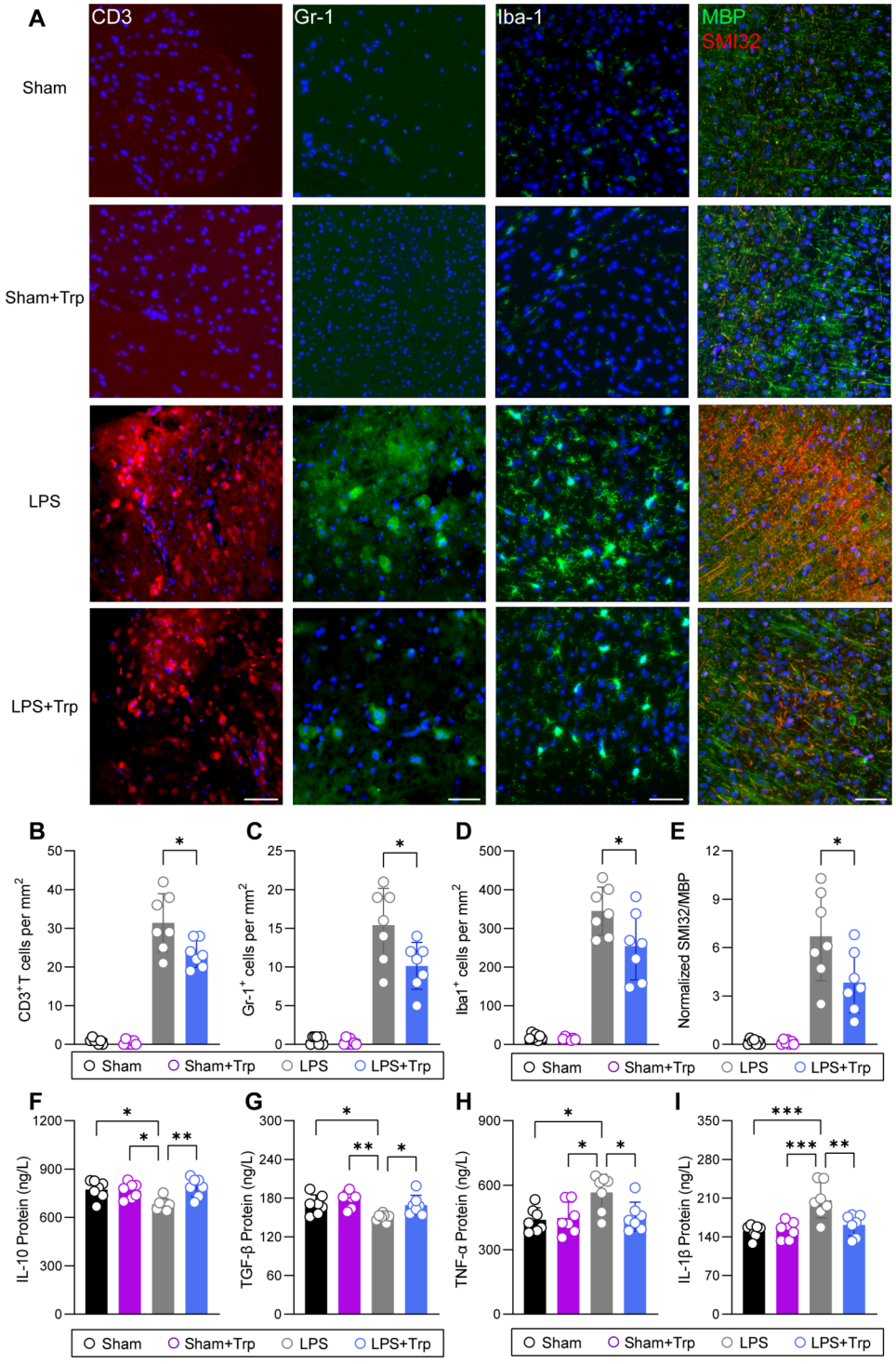

Fig. 3 Tryptophan-rich diet attenuated LPS-mediated neuroinflammation by activating Htr7$^+$ Tregs. **A** Representative images of CD3, Gr-1, Iba-1, and MBP immunostaining accompanied by SMI32 staining in the hippocampal DG 24 h after LPS treatment. Scale bar = 50 μm. **B-D** Quantification of CD3$^+$ (**B**), Gr-1$^+$ (**C**), and Iba-1$^+$ cells (**D**) ($n = 7$/group). **E** Normalized SMI32/MBP ratio ($n = 7$/group). **F-I** Levels of IL-10 (**F**), TGF-β (**G**), TNF-α (**H**), and IL-1β (**I**) in the hippocampus ($n = 7$/group). $^*P < 0.05$, $^{**}P < 0.01$, $^{***}P < 0.001$, ns indicates nonsignificant

label primary $CD8^+$ T cells to track their proliferation after co-culture with primary Tregs for 72 h. Figure 4A depicted representative dot plots from flow cytometry showing CFSE-labeled $CD8^+$ T cells that have undergone 1–2 cell divisions. Flow cytometry analysis revealed that in the first generation of CFSE-labeled $CD8^+$ T cells (P1), the proportion of $CD8^+$ T cells in the 5-HT group was significantly higher than that in the other two groups ($F_{(2,\ 15)}=11.66$, $P=0.0009$). However, in the second generation (P2), the percentage of $CD8^+$ T cells in the 5-HT group was markedly lower than that in the other two groups ($F_{(2,\ 15)}=20.52$, $P<0.0001$). In contrast, no significant differences in the proportions of $CD8^+$ T cells were observed among the three groups in the third generation (P3) ($F_{(2,\ 15)}=0.4412$, $P=0.6513$, Fig. 4B). These findings indicated that the binding of 5-HT to 5-HT_7 receptor can enhance the inhibitory effect of Tregs on the proliferation of $CD8^+$ T cells. We also employed flow cytometry to assess the apoptosis of primary $CD8^+$ T cells cocultured with primary Tregs (Fig. 4C). The percentage of apoptotic $CD8^+$ T cells in the 5-HT group was significantly greater than that in the PBS group and 5-HT + SB group ($F_{(2,\ 18)}=12.37$, $P=0.0004$, Fig. 4D). Additionally, we evaluated the alteration in the cytotoxic capacity of $CD8^+$ T cells by assessing the expression of perforin (Prf) and granzyme B (GranzB). Similarly, compared with those in both the PBS group and the 5-HT + SB group, the relative expression of Prf mRNA in the 5-HT group was significantly lower ($F_{(2,\ 18)}=15.26$, $P=0.0001$, Fig. 4E). Moreover, compared with those in both the PBS group and the 5-HT + SB group, the relative expression levels of GranzB mRNA in the 5-HT group were lower ($F_{(2,\ 18)}=6.233$, $P=0.0088$, Fig. 4F). As depicted in Fig. 4G, the relative expression level of the Prf protein in the 5-HT group was markedly lower than that in the PBS group and the 5-HT + SB group ($F_{(2,\ 18)}=8.173$, $P=0.0030$, Fig. 4H). Similarly, compared with those in the PBS group and the 5-HT + SB group, the relative expression levels of the GranzB protein in the 5-HT group were significantly lower ($F_{(2,\ 18)}=6.664$, $P=0.0068$, Fig. 4G, I).

Primary microglia were subsequently isolated from neonatal mouse brains, and primary Tregs were isolated from lymph nodes and cocultured in a 12-well plate. These cells were also divided into PBS, 5-HT, and 5-HT + SB groups according to the different stimulus factors added to the medium. We employed flow cytometry to assess the polarization of primary microglia cocultured with primary Tregs. MHC-II was used as a marker of M1 polarization, and the mean fluorescence intensity (MFI) of MHC-II revealed a notable reduction in M1 polarization in the 5-HT group compared to both the PBS group and the 5-HT + SB group ($F_{(2,\ 18)}=8.428$, $P=0.0026$, Fig. 4J). Furthermore, CD206 was utilized as a marker of M2 polarization, and the MFI of CD206 indicated a substantial increase in M2 polarization in the 5-HT group compared with both the PBS group and the 5-HT + SB group ($F_{(2,\ 18)}=9.470$, $P=0.0015$, Fig. 4K). Furthermore, we assessed microglial immune function by examining the expression of inflammatory factor mRNAs in microglia. Compared to those in the PBS group and the 5-HT + SB group, the 5-HT group exhibited significant decreases in the mRNA levels of IL-1β ($F_{(2,\ 18)}=7.989$, $P=0.0033$, Fig. 4L). The relative expression level of IL-4 mRNA in the 5-HT group was significantly lower than that in both the PBS group and the 5-HT + SB group ($F_{(2,\ 18)}=8.400$, $P=0.0026$, Fig. 4M). Moreover, compared with those in both the PBS group and the 5-HT + SB group, the relative expression levels of inducible nitric oxide synthase (iNOS) mRNA in the 5-HT group were significantly lower ($F_{(2,\ 18)}=6.866$, $P=0.0061$, Fig. 4N). Similarly, the mRNA levels of TNF-α were significantly lower in the 5-HT group than in both the PBS group and the 5-HT + SB group ($F_{(2,\ 18)}=11.33$, $P=0.0007$, Fig. 4O).

These findings showed that primary $Htr7^+$ Tregs exert immunosuppressive effects on primary $CD8^+$ T cells and primary microglia by binding to 5-HT and the 5-HT_7 receptor on the cell surface.

Htr7+ Tregs alleviated LPS-induced cognitive impairment in Rag1-/- mice

We further examined whether $Htr7^+$ Tregs mitigated neuroinflammation-induced cognitive impairment (Fig. 5A). After isolating and transfecting the lentivirus to downregulate Htr7 in the cervical lymph nodes of healthy C57BL/6 mice, we confirmed the significant reduction in Htr7 in Tregs through HPLC–MS analysis ($t_{(12)}=5.428$, $P=0.0002$, Fig. 5B). Subsequently, 2×10^6 transfected Tregs and $CD4^+CD25^-$ T cells were intravenously injected into recipient $Rag1^{-/-}$ mice. $Rag1^{-/-}$ mice lack mature T and B cells, preventing consideration of the impact of other T and B lymphocytes on the experiment. The cervical lymph nodes of $Rag1^{-/-}$ mice was collected for flow cytometry analysis of $CD4^+$ T lymphocytes and Tregs levels. Figure 5C showed that there were very few $CD4^+$ T lymphocytes and Tregs in the cervical lymph nodes of $Rag1^{-/-}$ mice, demonstrating the successful establishment of $Rag1^{-/-}$ immunodeficient mouse model. The results suggested that the levels of $CD4^+$ T lymphocytes and Tregs in the cervical lymph nodes of $Rag1^{-/-}$ mice without Tregs and $CD4CD25^-$ T-cell infusion were significantly lower than those in the Tregs infusion group ($t_{(12)}=0.8154$, $P=0.4307$, Fig. 5D, E). These results indicated that lentivirus-transfected Tregs were viable and the adoptive transferred Tregs survived successfully in $Rag1^{-/-}$ mice.

The MWM training was performed 24 h after femoral vein injection. The MWM training results revealed

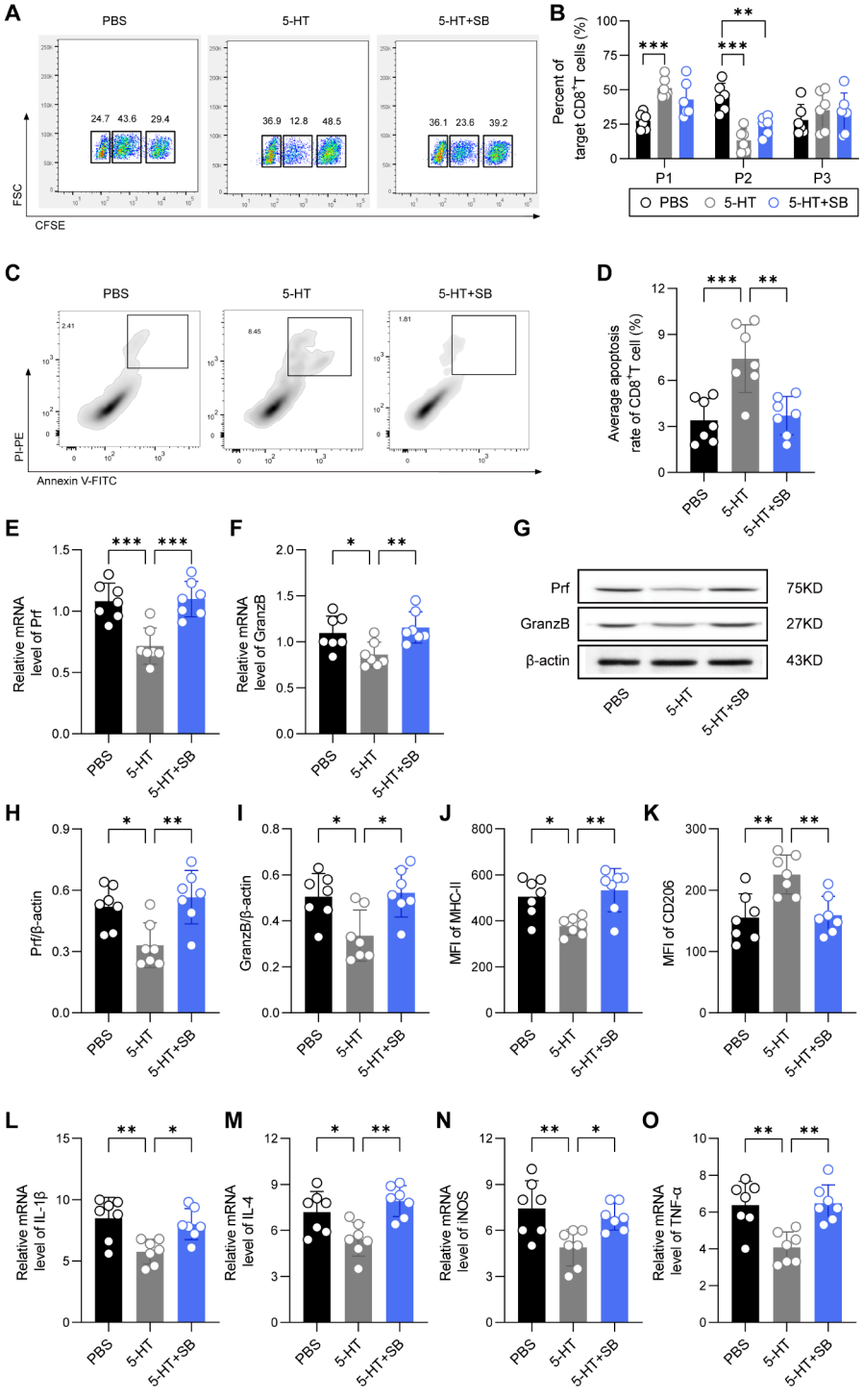

Fig. 4 5-HT and 5-HT$_7$ receptor enhanced the immunosuppressive effect of Tregs on CD8$^+$ T cells and microglia. **A** Representative dot plots of flow cytometry analysis of CFSE-positive primary CD8$^+$ T cells in cervical lymph nodes. **B** Quantification of the percentage of target CD8$^+$ T cells at different time points. **C** Representative flow cytometry dot plots showing apoptosis in primary CD8$^+$ T cells in cervical lymph nodes. **D** Quantification of the percentage of apoptotic primary CD8$^+$ T cells. **E**, **F** mRNA levels of the cytokines perforin (Prf) (**E**) and granzyme B (GranzB) (**F**), as measured by qRT-PCR. **G** Representative Western blot images of Prf and GranzB. **H**, **I** Quantification of the relative expression of the Prf protein (**H**) and the GranzB protein (**I**). **J-K** Mean fluorescence intensity (MFI) of MHC-II$^+$ (**J**) and CD206$^+$ cells (**K**). **L-O** mRNA levels of IL-1β (**L**), IL-4 (**M**), iNOS (**N**), and TNF-α (**O**). $^*P<0.05$, $^{**}P<0.01$, $^{***}P<0.001$, ns indicates nonsignificant

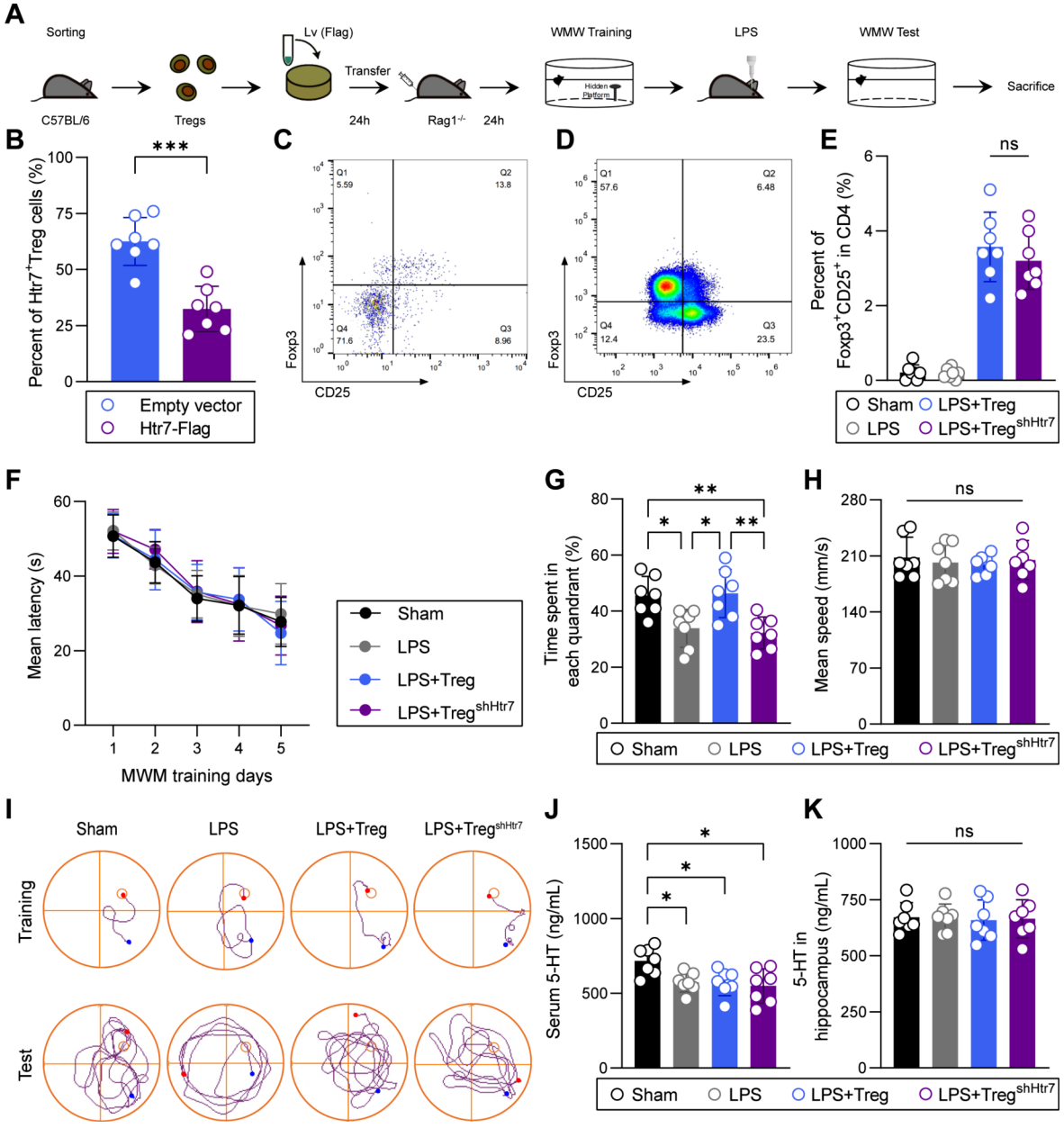

Fig. 5 Htr7^{+} Tregs alleviated LPS-induced cognitive impairment and decreased peripheral 5-HT in Rag1$^{-/-}$ mice. **A** Flowchart illustrates the experimental design. **B** Htr7 levels in Tregs transfected with lentiviral downregulation of Hr7 ($n=7$/group). **C** Representative dot plots of Tregs detected via flow cytometry in the cervical lymph nodes of Rag1$^{-/-}$ mice ($n=7$/group). **D**, **E** Representative dot plots and the percentages of Tregs detected via flow cytometry in the cervical lymph nodes of Rag1$^{-/-}$ mice with adoptively transferred Tregs transfected with the Htr7-Flag lentivirus ($n=7$/group). **F** Mean escape latency to reach the hidden platform during the 5-day training ($n=7$/group). **G** The percentage of time spent in the target quadrant ($n=7$/group). **H** The mean swimming velocity exhibited by each experimental group during the probe test ($n=7$/group). **I** Representative trace graphs during the MWM test. **J**, **K** Serum 5-HT and hippocampal 5-HT concentrations in the peripheral blood of mice after LPS treatment ($n=7$/group). $^{*}P<0.05$, $^{**}P<0.01$, $^{***}P<0.001$, ns indicates nonsignificant

an increase in the proficiency of the mice in locating the concealed platform during the training phase, with no discernible differences in the daily latency to reach the platform across the groups ($F_{(3,\ 24)}=0.1867$, $P=0.9044$, Fig. 5F, I). The probe test was conducted 24 h after LPS administration, during which all four groups of mice demonstrated a notable preference for the target quadrant, in which they spent significantly more time in the target quadrant than in the opposite quadrant. Notably, the LPS group and LPS+Treg^{shHtr7} group exhibited a distinct decrease in the duration spent in the target quadrant, setting them apart from the other two groups ($F_{(3,\ 24)}=7.875$, $P=0.0008$, Fig. 5G, I). The swimming velocities displayed by the mice were comparable across

all groups, effectively excluding any potential effect of motor or perceptual factors on spatial learning and memory ($F_{(3, 24)}$=0.1774, P=0.9106, Fig. 5H). These findings suggested that Htr7$^+$ Tregs mitigate the deleterious effects of LPS-induced cognitive impairment in mice.

The HPLC–MS technique was also used to evaluate the levels of 5-HT in the peripheral blood and hippocampal regions of mice following intracerebroventricular injection. The results revealed that, in comparison with those in the Sham group, the other three groups exhibited markedly lower levels of 5-HT in the peripheral blood ($F_{(3, 24)}$=5.024, P=0.0076, Fig. 5J). Furthermore, there was no significant disparity in the concentration of 5-HT in the hippocampal region among the four groups of mice ($F_{(3, 24)}$=0.0363, P=0.9905, Fig. 5K). These findings were consistent with the outcomes of previous experiments, indicating that intracerebroventricular injection of LPS disrupted 5-HT biosynthesis.

Htr7+ Tregs ameliorated LPS-induced neuroinflammation in Rag1-/- mice

The preceding findings demonstrated that in Rag1$^{-/-}$ mice, Htr7$^+$ Tregs alleviated LPS-induced cognitive impairment and decreased peripheral 5-HT levels. However, whether Htr7$^+$ Tregs achieve this effect by mitigating central inflammation remains to be elucidated. Therefore, flow cytometry was used to evaluate the expression of CD206$^+$ and MHC-II$^+$ microglia in the hippocampus 24 h after LPS treatment (Fig. 6A). In the LPS and LPS+Treg^{shHtr7} groups, the expression of CD206$^+$ microglia in the hippocampus was lower than that in the other two groups ($F_{(3, 24)}$=9.930, P=0.0002, Fig. 6B). Moreover, the number of MHC-II$^+$ microglia in the hippocampus of mice in the LPS and LPS+Treg^{shHtr7} groups was significantly greater than that in the other two groups ($F_{(2, 18)}$=11.71, P=0.0006, Fig. 6C). Moreover, the expression of CD206$^+$ macrophage in the hippocampal tissue of mice in the LPS group was lower than that in the Sham and LPS+Treg groups ($F_{(3, 24)}$=7.313, P=0.0012, Fig. 6D). Similarly, the number of MHC-II$^+$ macrophage in the hippocampal tissue of mice in the LPS and LPS+Treg^{shHtr7} groups was greater than that in the other two groups ($F_{(2, 18)}$=9.601, P=0.0015, Fig. 6E). We also found that the upregulation of MHC-I$^+$ microglia ($F_{(2, 18)}$=7.583, P=0.0041) and MHC-I$^+$ macrophage ($F_{(2, 18)}$=5.511, P=0.0136) in the hippocampal tissue of mice in the LPS and LPS+Treg^{shHtr7} groups was evident in comparison to that in the other two groups (Fig. 6F, G). These results demonstrated that Htr7$^+$ Tregs promote the protective polarization of microglia and macrophages in Rag1$^{-/-}$ mice. Notably, immunofluorescence staining of the hippocampal DG region revealed enhanced Iba-1 staining in the LPS group and LPS+Treg^{shHtr7} group compared to the other two groups, which similarly indicated a significant increase in microglial activation ($F_{(3, 24)}$=12.54, P<0.0001, Fig. 6H, I). We employed ELISA to evaluate the levels of inflammatory factors in the hippocampal region. Compared to those in the other two groups, the IL-10 levels in the hippocampal region were lower in the LPS group and the LPS+Treg^{shHtr7} group ($F_{(3, 24)}$=11.05, P<0.0001, Fig. 6J). Similarly, in contrast to those in the Sham group, the LPS+Treg^{shHtr7} group exhibited a notable reduction in the hippocampal TGF-β concentration ($F_{(3, 24)}$=4.654, P=0.0106, Fig. 6K). Moreover, the LPS+Treg^{shHtr7} group displayed a substantial increase in TNF-α levels in the hippocampal region compared to those in the Sham and LPS+Treg groups ($F_{(3, 24)}$=4.493, P=0.0122, Fig. 6L). Additionally, the LPS+Treg^{shHtr7} group exhibited significantly greater IL-1β levels in the hippocampal region than did the Sham and LPS+Treg groups ($F_{(3, 24)}$=4.995, P=0.0078, Fig. 6M). These findings indicated that Htr7$^+$ Tregs alleviate cognitive dysfunction by mitigating central inflammation.

Discussion

In this study, we focused on neuroinflammation-induced cognitive impairment and demonstrated that Htr7$^+$ Tregs alleviate cognitive dysfunction by inhibiting central nervous system inflammatory responses. Our research results provide scientific evidence for the role of Htr7$^+$ Tregs in alleviating neuroinflammation caused by various factors.

The pathogenesis of cognitive dysfunction involves multiple mechanisms, such as neuroinflammation, oxidative stress, and neurodegenerative changes [18–21]. Tregs play a pivotal role in the intricate process of effector T cell suppression, thereby maintaining self-tolerance and ensuring immune system homeostasis [22]. Moreover, the impairment of Tregs under neurodegenerative conditions leads to a loss of inflammation, ultimately resulting in the persistence of inflammatory environments within the central nervous system. This study investigated the impact of Htr7$^+$ Tregs on neuroinflammation and inflammation-related memory impairment in a mouse model of LPS-treatment.

Our study found that 5-HT levels were reduced in peripheral blood and colon tissues of mice subjected to LPS treatment, yet the underlying mechanisms remain elusive. 5-HT, predominantly synthesized in the enteric system, arises from the metabolic conversion of tryptophan, an essential amino acid derived from dietary intake, into serotonin. This transformation is orchestrated by the enzyme tryptophan hydroxylase 1 (TPH1), which serves as the rate-limiting catalyst in the biosynthetic pathway of 5-HT [23]. Studies have indicated that, compared to specific pathogen-free mice, germ-free mice exhibit a significant reduction in the expression levels of TPH1, the rate-limiting enzyme in the 5-HT synthesis pathway, in

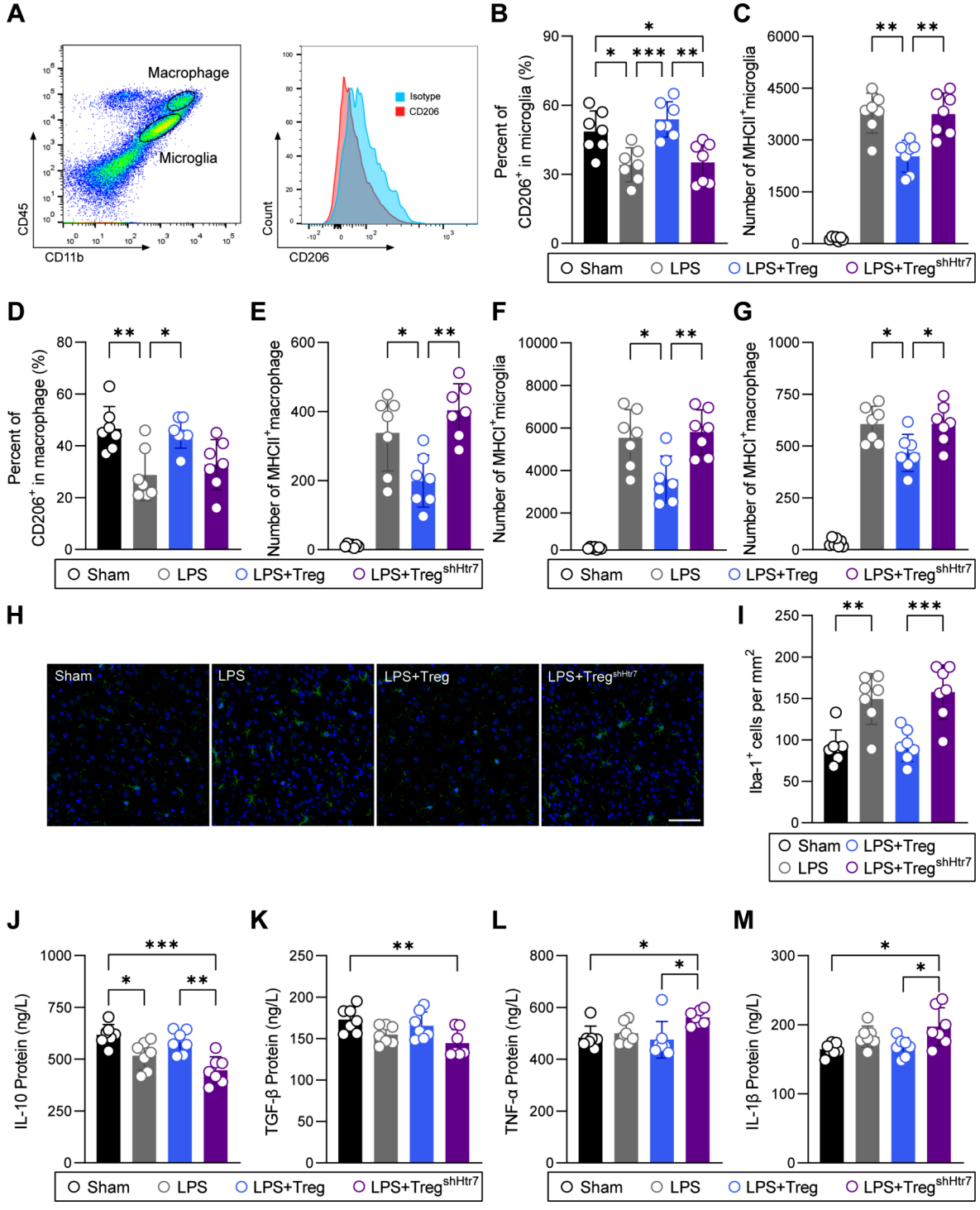

Fig. 6 Htr7$^+$ Tregs ameliorated LPS-induced neuroinflammation in Rag1$^{-/-}$ mice. **A** Representative dot plots of CD206$^+$ microglia in the hippocampus of Rag1$^{-/-}$ mice adoptively transferred to Tregs transfecting with the lentivirus Htr7-Flag ($n=7$/group). **B** Percent of flow cytometry data for CD206$^+$ microglia in the hippocampus of Rag1$^{-/-}$ mice ($n=7$/group). **C** Absolute number of MHC-II$^+$ microglia in the hippocampus of Rag1$^{-/-}$ mice ($n=7$/group). **D** Percent of CD206$^+$ macrophage in the hippocampus of Rag1$^{-/-}$ mice determined by flow cytometry ($n=7$/group). **E** Absolute number of MHC-II$^+$ macrophage in the hippocampus of Rag1$^{-/-}$ mice ($n=7$/group). **F** Absolute number of MHC-I$^+$ microglia in the hippocampus of Rag1$^{-/-}$ mice ($n=7$/group). **G** Absolute number of MHC-I$^+$ macrophage in the hippocampus of Rag1$^{-/-}$ mice ($n=7$/group). **H** Representative images of Iba-1 immunostaining in the hippocampal DG of Rag1$^{-/-}$ mice with adoptively transferred Tregs transfecting with the lentivirus Htr7-Flag. Scale bar = 50 μm. **I** Quantification of Iba-1$^+$ cells ($n=7$/group). **J-M** Levels of IL-10 (**J**), TGF-β (**K**), TNF-α (**L**), and IL-1β (**M**) in the hippocampal DG of Rag1$^{-/-}$ mice adoptively transferred into Tregs and transfected with the lentivirus Htr7-Flag. ($n=7$/group). $^*P<0.05$, $^{**}P<0.01$, $^{***}P<0.001$, ns indicates nonsignificant

the colon [24]. Additionally, research has confirmed that short-chain fatty acids (SCFAs), such as isovaleric acid, produced by the gut microbiota through the fermentation of cellulose, can activate voltage-gated ion channels in enterochromaffin cells, thereby promoting the release of intracellular 5-HT [25]. It is possible that neuroinflammation and gut microbiota interact through the gut-brain axis. The current study offers a foundational direction for subsequent inquiries into the role of the gut microbiota and its potential to modulate neuroinflammation-associated cognitive impairments.

Tregs, by their ability to abrogate the pathogenic activities of immune cells and sustain immunological tolerance toward self-antigens, have garnered considerable attention over the years. Tregs exert immune suppressive effects through three main pathways: (1) inhibiting cytokine production or promoting effector T cell proliferation; (2) engaging in the direct secretion of cytokines, notably TGF-β and IL-10, thus orchestrating the cytokine milieu at the inflammatory site; and (3) directly killing cytotoxic cells [26]. Based on the systematic study of Tregs by Minako et al. [13], we proposed that the reduced activation of $Htr7^+$ Tregs is due to a decrease in peripheral blood 5-HT levels. Consequently, when we increased the peripheral blood 5-HT concentration by providing the diet rich in tryptophan, we observed a significant improvement in cognitive function in mice following intracerebroventricular microinjection of LPS. Building upon the comprehensive investigation of Tregs by Minako et al. [13], we posited that the diminished activation of $Htr7^+$ Tregs stems from reduced peripheral blood 5-HT levels, while augmenting peripheral blood 5-HT can stimulate the proliferation and activation of $Htr7^+$ Tregs. Thus, we observed that mice receiving the tryptophan-rich diet to increase peripheral blood 5-HT levels after intracerebroventricular injection of LPS exhibited significantly greater proportions of $Htr7^+$ Tregs in the cervical lymph nodes and hippocampus than mice receiving only intracerebroventricular injection of LPS. Additionally, there was an elevation in central anti-inflammatory factor levels, a reduction in inflammatory cell and proinflammatory factor levels, and alleviation of demyelination in neurons. Moreover, the cognitive function of the mice improved.

Current evidence suggests the potential interplay between immune dysregulation and cognitive decline in individuals with mild cognitive impairment or mild AD. Studies have revealed elevated levels of activated $CD4^+$ T and $CD8^+$ T cells in these individuals, indicating an aberrant immune response [27]. Notably, increased activation of $CD8^+$ T cells has been linked to compromised language acquisition, visual-spatial abilities, and hippocampal degradation, which are hallmark features of cognitive impairment [28]. This finding points toward a potential association between the cognitive manifestations of AD and the heightened activation of $CD8^+$ T cells. Furthermore, investigations have shown elevated quantities of effector memory $CD8^+$ T cells in the CSF of AD patients, highlighting their involvement in central inflammation [29]. Previous investigations conducted by our research group and other scholars have revealed notable infiltration of $CD8^+$ T cells within the cerebral parenchyma of mice afflicted with ischemic stroke. These $CD8^+$ T-cell-derived Prf and GranzB compounds have been determined to play a significant role in neurotoxicity, exacerbating perioperative ischemic brain injury and subsequently leading to cognitive impairment [11, 30]. These findings suggested that $CD8^+$ T cells play a pivotal role in mediating inflammation and cognitive impairment. In coculture experiments, 5-HT was shown to enhance the immunosuppressive effect of primary Tregs on primary $CD8^+$ T cells through activation of the $5\text{-}HT_7$ receptor. These findings indicated that 5-HT amplifies the immunosuppressive effects of Tregs on primary $CD8^+$ T cells through the activation of the $5\text{-}HT_7$ receptor.

The activation of microglia plays a key role in promoting neuroinflammation, a process implicated in various neurological disorders [31]. Currently, an increasing number of studies are related to the M1/M2 paradigm of microglial activation, wherein the M1 phenotype of microglia represents a proinflammatory state, while the M2 phenotype embodies an anti-inflammatory state [32]. Notably, exposure of microglia to LPS and sevoflurane, a commonly used anesthetic, stimulates the expression of the proinflammatory cytokines IL-1β and IL-6 [33]. Similarly, the administration of isoflurane, another anesthetic, has been shown to promote microglial inflammation and induce cognitive decline in elderly mice [34]. In an effort to mitigate these detrimental effects, researchers have focused on upregulating the expression of IL-10 in microglia, which can inhibit the NF-κB/MAPK pathway and alleviate postoperative cognitive dysfunction (POCD) [35]. Additionally, the activation of 5-HT receptors has emerged as a promising strategy for limiting neuroinflammation. By reducing astrocyte and microglial reactivity, 5-HT receptor activation protects the brain from inflammation-induced neurodegenerative changes [36, 37]. The aforementioned studies primarily concentrated on the activation of hippocampal 5-HT receptors. In the present study, we investigated the importance of $5\text{-}HT_7$ receptors positioned on the surface of peripheral Tregs. We cocultured primary Tregs with primary microglia and found that in the 5-HT group, microglia exhibited a decrease in M1 polarization, which enhanced the inflammatory response, and an increase in M2 polarization, which promoted neural repair. Furthermore, the 5-HT group exhibited significant decreases in the concentrations of IL-1β and TNF-α. However, when

5-HT and 5-HT_7 receptor antagonists were added to the culture medium, this enhanced immunosuppressive effect was blocked. These findings suggested that 5-HT enhances the immunosuppressive effect of primary Tregs on primary microglia through the 5-HT_7 receptor.

The addition of 5-HT to culture media enhances the immunosuppressive effects of primary Tregs on cocultured primary $CD8^+$ T cells and primary microglia. However, the simultaneous addition of 5-HT and a 5-HT_7 receptor antagonist to the culture medium abolished the suppressive effects of primary $CD8^+$ T cells and primary microglia on cocultured primary Tregs. These findings further substantiated the crucial immunomodulatory role of $Htr7^+$ Tregs.

$Rag1^{-/-}$ mice lack mature T and B cells. Following intravenous injection of primary Tregs, the impact of Tregs on neuroinflammation and cognitive function in $Rag1^{-/-}$ mice can be observed independently, thereby eliminating interference from other T and B lymphocytes. By selectively transferring $Htr7^+$ Tregs into $Rag1^{-/-}$ mice in vivo, the attenuation of Htr7 expression on the surface of $Htr7^+$ Tregs intensified the cognitive impairment and neuroinflammatory responses induced by the administration of LPS. These data support our conclusion that $Htr7^+$ Tregs can alleviate the cognitive impairments caused by LPS-induced neuroinflammation (Fig. 7).

There are several limitations in our study. First, central nervous system inflammation is a complex pathological process involving many immune cells from both the central and peripheral tissues. The current study is solely focused on $Htr7^+$ Tregs in cervical lymph nodes and brain. Future research should employ single-cell RNA sequencing to examine the status of various cell populations in peripheral lymph nodes and brain tissues. Second, the pathogenesis cognitive impairment caused by neurodegenerative diseases is complex. Although neuroinflammation is one of the major contributing factors, aging is still one of the factors that cannot be ignored. It would be beneficial to conduct further investigations using aged animal models. Third, the disruption of gut microbiota secondary to neuroinflammation through gut-brain axis may be a significant factor contributing to the observed decline in 5-HT levels in peripheral blood

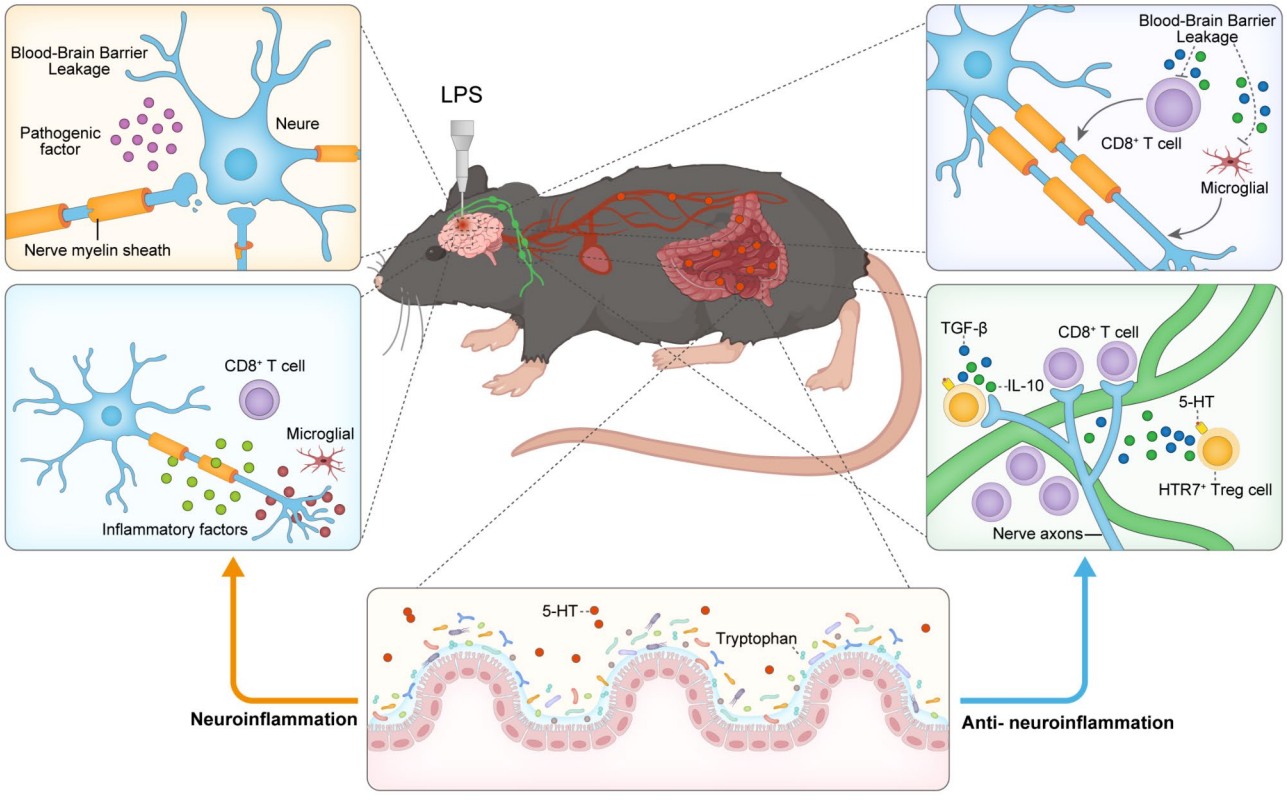

Fig. 7 The schematic illustration depicts the effects of the tryptophan-rich diet on $Htr7^+$ Tregs in alleviating neuroinflammation and cognitive impairment induced by lipopolysaccharide. Decreased peripheral blood 5-HT levels after intracerebroventricular administration of LPS resulted in decreased proliferation and activation of $HTR7^+$ Tregs and led to decreased infiltration of $HTR7^+$ Tregs and Tregs-derived immunosuppressive factors into the hippocampal region in the cervical lymph nodes. This further leads to increased activation of damaging peripheral immune cells, inflammatory mediators, and microglia in the hippocampus, ultimately leading to cognitive dysfunction. Administration of the tryptophan-rich diet elevated peripheral blood 5-HT levels to activate $HTR7^+$ Tregs, thereby reducing the inflammatory response in the hippocampus and mitigating cognitive dysfunction

and colon tissues post-LPS intracerebroventricular injection. Future studies should endeavor to elucidate the specific mechanisms by which neuroinflammation induces a decrease in 5-HT in the peripheral blood and colon tissues.

Conclusions

In conclusion, our study demonstrated the pivotal role of $Htr7^+$ Tregs in LPS-induced cognitive impairment, suggesting that $Htr7^+$ Tregs may be critical for alleviating central inflammation-associated cognitive impairment. $Htr7^+$ Tregs alleviated the inflammatory response and prevent neuronal damage by suppressing the infiltration of $CD8^+$ T cells into the brain and excessive activation of microglia, thereby ameliorating LPS-induced cognitive impairment. This study may offer new potential therapeutic targets based on Tregs for neuroinflammation-mediated cognitive dysfunction.

Abbreviations

Tregs	Regulatory T cells
LPS	Lipopolysaccharide
5-HT	5-hydroxytryptamine
APCs	Antigen-presenting cells
HPLC–MS	High-performance liquid chromatography–mass spectrometry
Trp	Tryptophan
Rag1	Recombination activating gene 1
aCSF	artificial cerebrospinal fluid
MWM	Morris water maze
OF	Open filed
SYN	Synephrine
DHBA	Dihydroxybenzylamine
CFSE	Carboxyfluorescein diacetate succinimidyl ester
PI	Propidium iodide
Prf	Perforin
GranzB	Granzyme B
MBP	Myelin basic protein
SB	SB269970
DG	Dentate gyrus
TPH1	Tryptophan hydroxylase 1
SCFAs	Short-chain fatty acids
iNOS	Inducible nitric oxide synthase
MFI	Mean fluorescence intensity
POCD	Postoperative cognitive disorders

Acknowledgements
We thank Haodong Zhao for his assistance during the image processing procedure.

Author contributions
Conceptualization, LW and QF; Data curation, YXL and LYL; Funding acquisition, LW and QF; Methodology, DHX, XG and JJL; Project administration, LW and QF; Resources, JBC and YHL; Software, YXL, LYL and MRZ; Validation, GSL and MRZ; Writing – original draft, DHX, XG and JJL; Writing – review & editing, JSL, HL and WDM.

Funding
The present research was supported by the National Natural Science Foundation of China (No. 82071178, 82271322).

Data availability
No datasets were generated or analysed during the current study.

Declarations

Ethics approval and consent to participate
All animal experiments were performed in accordance with the National Institute of Health Guide for Care and Use of Laboratory Animals, with the approval of the Ethics Committee for Animal Experimentation of the Chinese PLA General Hospital.

Consent for publication
Not applicable.

Competing interests
The authors declare no competing interests.

Author details
[1]Department of Anesthesiology, The First Medical Center, Chinese PLA General Hospital, Beijing 100853, China
[2]Department of Anesthesiology, Beijing Tongren Hospital, Capital Medical University, Beijing 100730, China
[3]Department of Anesthesiology, Chinese People's Armed Police Force Hospital of Beijing, Beijing 100027, China
[4]Department of Anesthesiology, The 71st Group Army Hospital of CPLA Army, Xuzhou 221004, China
[5]Department of Pain Medicine, The First Medical Center, Chinese PLA General Hospital, Beijing 100853, China

Received: 23 January 2024 / Accepted: 23 September 2024
Published online: 27 September 2024

References

1. Liang X, Xue Z, Zheng Y, Li S, Zhou L, Cao L, et al. Selenium supplementation enhanced the expression of selenoproteins in hippocampus and played a neuroprotective role in LPS-induced neuroinflammation. Int J Biol Macromol. 2023;234:123740.
2. Kim HS, Kim S, Shin SJ, Park YH, Nam Y, Kim CW, et al. Gram-negative bacteria and their lipopolysaccharides in Alzheimer's disease: pathologic roles and therapeutic implications. Transl Neurodegener. 2021;10:49.
3. Zhou Y, Ju H, Hu Y, Li T, Chen Z, Si Y, et al. Tregs dysfunction aggravates postoperative cognitive impairment in aged mice. J Neuroinflammation. 2023;20:75.
4. Wang L, Zhou Y, Yin J, Gan Y, Wang X, Wen D, et al. Cancer exacerbates ischemic brain Injury Via Nrp1 (Neuropilin 1)-Mediated Accumulation of Regulatory T Cells within the Tumor. Stroke. 2018;49:2733–42.
5. Ma G, Chen C, Jiang H, Qiu Y, Li Y, Li X et al. Ribonuclease attenuates hepatic ischemia reperfusion induced cognitive impairment through the inhibition of inflammatory cytokines in aged mice. Biomedicine & Pharmacotherapy = Biomedecine & Pharmacotherapie. 2017;90:62–8.
6. Luo A, Yan J, Tang X, Zhao Y, Zhou B, Li S. Postoperative cognitive dysfunction in the aged: the collision of neuroinflammaging with perioperative neuroinflammation. Inflammopharmacology. 2019;27:27–37.
7. Liang Y, Kang X, Zhang H, Xu H, Wu X. Knockdown and inhibition of hippocampal GPR17 attenuates lipopolysaccharide-induced cognitive impairment in mice. J Neuroinflamm. 2023;20:271.
8. Kim J, Lee H-J, Park J-H, Cha B-Y, Hoe H-S. Nilotinib modulates LPS-induced cognitive impairment and neuroinflammatory responses by regulating P38/STAT3 signaling. J Neuroinflammation. 2022;19:187.
9. Sun M, Li Y, Liu M, Li Q, Shi L, Ruan X, et al. Insulin alleviates lipopolysaccharide-induced cognitive impairment via inhibiting neuroinflammation and ferroptosis. Eur J Pharmacol. 2023;955:175929.
10. Barbi J, Pardoll D, Pan F. Treg functional stability and its responsiveness to the microenvironment. Immunol Rev. 2014;259:115–39.
11. Zhang F, Niu M, Guo K, Ma Y, Fu Q, Liu Y, et al. The immunometabolite S-2-hydroxyglutarate exacerbates perioperative ischemic brain injury and cognitive dysfunction by enhancing CD8 + T lymphocyte-mediated neurotoxicity. J Neuroinflammation. 2022;19:176.
12. Tian A, Ma H, Cao X, Zhang R, Wang X, Wu B. Vitamin D improves cognitive function and modulates Th17/T reg cell balance after hepatectomy in mice. Inflammation. 2015;38:500–9.

13. Ito M, Komai K, Mise-Omata S, Iizuka-Koga M, Noguchi Y, Kondo T, et al. Brain regulatory T cells suppress astrogliosis and potentiate neurological recovery. Nature. 2019;565:246–50.
14. Margolis KG, Cryan JF, Mayer EA. The Microbiota-Gut-Brain Axis: from motility to Mood. Gastroenterology. 2021;160:1486–501.
15. Wang D, Wu J, Zhu P, Xie H, Lu L, Bai W, et al. Tryptophan-rich diet ameliorates chronic unpredictable mild stress induced depression- and anxiety-like behavior in mice: the potential involvement of gut-brain axis. Food Res Int. 2022;157:111289.
16. Nemoto W, Kozak D, Sotocinal SG, Tansley S, Bannister K, Mogil JS. Monoaminergic mediation of hyperalgesic and analgesic descending control of nociception in mice. Pain. 2023;164:1096–105.
17. Zhao W, Xu Z, Cao J, Fu Q, Wu Y, Zhang X, et al. Elamipretide (SS-31) improves mitochondrial dysfunction, synaptic and memory impairment induced by lipopolysaccharide in mice. J Neuroinflamm. 2019;16:230.
18. Sun L, Yong Y, Wei P, Wang Y, Li H, Zhou Y, et al. Electroacupuncture ameliorates postoperative cognitive dysfunction and associated neuroinflammation via NLRP3 signal inhibition in aged mice. CNS Neurosci Ther. 2022;28:390–400.
19. Netto MB, De Oliveira Junior AN, Goldim M, Mathias K, Fileti ME, Da Rosa N et al. Oxidative stress and mitochondrial dysfunction contributes to postoperative cognitive dysfunction in elderly rats. Brain, Behavior, and Immunity. 2018;73:661–9.
20. Granger KT, Barnett JH. Postoperative cognitive dysfunction: an acute approach for the development of novel treatments for neuroinflammation. Drug Discovery Today. 2021;26:1111–4.
21. Kant IMJ, De Bresser J, Van Montfort SJT, Slooter AJC, Hendrikse J. MRI markers of neurodegenerative and neurovascular changes in relation to postoperative Delirium and Postoperative Cognitive decline. Am J Geriatr Psychiatry. 2017;25:1048–61.
22. Ohkura N, Sakaguchi S. Transcriptional and epigenetic basis of Treg cell development and function: its genetic anomalies or variations in autoimmune diseases. Cell Res. 2020;30:465–74.
23. Höglund E, Øverli Ø, Winberg S. Tryptophan metabolic pathways and brain serotonergic activity: a comparative review. Front Endocrinol. 2019;10:158.
24. Roussin L, Gry E, Macaron M, Ribes S, Monnoye M, Douard V, et al. Microbiota influence on behavior: integrative analysis of serotonin metabolism and behavioral profile in germ-free mice. FASEB J. 2024;38:e23648.
25. Bellono NW, Bayrer JR, Leitch DB, Castro J, Zhang C, O'Donnell TA, et al. Enterochromaffin Cells Are Gut Chemosensors that couple to sensory neural pathways. Cell. 2017;170:185–e19816.
26. Yang Z, Yu A, Liu Y, Shen H, Lin C, Lin L, et al. Regulatory T cells inhibit microglia activation and protect against inflammatory injury in intracerebral hemorrhage. Int Immunopharmacol. 2014;22:522–5.
27. Reagin KL, Funk KE. The role of antiviral CD8 + T cells in cognitive impairment. Curr Opin Neurobiol. 2022;76:102603.
28. Lueg G, Gross CC, Lohmann H, Johnen A, Kemmling A, Deppe M, et al. Clinical relevance of specific T-cell activation in the blood and cerebrospinal fluid of patients with mild Alzheimer's disease. Neurobiol Aging. 2015;36:81–9.
29. Gate D, Saligrama N, Leventhal O, Yang AC, Unger MS, Middeldorp J, et al. Clonally expanded CD8 T cells patrol the cerebrospinal fluid in Alzheimer's disease. Nature. 2020;577:399–404.
30. Lee PR, Johnson TP, Gnanapavan S, Giovannoni G, Wang T, Steiner JP, et al. Protease-activated receptor-1 activation by granzyme B causes neurotoxicity that is augmented by interleukin-1β. J Neuroinflamm. 2017;14:131.
31. Leng F, Edison P. Neuroinflammation and microglial activation in Alzheimer disease: where do we go from here? Nat Rev Neurol. 2021;17:157–72.
32. Lee JH, Kam EH, Kim SY, Cheon SY, Kim EJ, Chung S, et al. Erythropoietin attenuates postoperative cognitive dysfunction by shifting macrophage activation toward the M2 phenotype. Front Pharmacol. 2017;8:839.
33. Ye X, Lian Q, Eckenhoff MF, Eckenhoff RG, Pan JZ. Differential general anesthetic effects on microglial cytokine expression. PLoS ONE. 2013;8:e52887.
34. Wang Z, Meng S, Cao L, Chen Y, Zuo Z, Peng S. Critical role of NLRP3-caspase-1 pathway in age-dependent isoflurane-induced microglial inflammatory response and cognitive impairment. J Neuroinflamm. 2018;15:109.
35. Zhang D, Li N, Wang Y, Lu W, Zhang Y, Chen Y, et al. Methane ameliorates post-operative cognitive dysfunction by inhibiting microglia NF-κB/MAPKs pathway and promoting IL-10 expression in aged mice. Int Immunopharmacol. 2019;71:52–60.
36. Bokobza C, Jacquens A, Guenoun D, Bianco B, Galland A, Pispisa M, et al. Targeting the brain 5-HT7 receptor to prevent hypomyelination in a rodent model of perinatal white matter injuries. J Neural Transm. 2023;130:281–97.
37. Costa L, Tempio A, Lacivita E, Leopoldo M, Ciranna L. Serotonin 5-HT7 receptors require cyclin-dependent kinase 5 to rescue hippocampal synaptic plasticity in a mouse model of Fragile X Syndrome. Eur J Neurosci. 2021;54:4124–32.

Publisher's note